REPORT DOCUMENTATION PAGE

2 9 NOV 1999

AFRL-SR-BL-TR-99-

0280

Public reporting burden for this collection of information is estimated to average 1 hour per response, including the time the data needed, and completing and reviewing this collection of information. Send comments regarding this burden es reducing this burden to Washington Headquarters Services, Directorate for Information Operations and Reports, 1215 J Management and Budget, Paperwork Reduction Project (0704-0188), Washington, DC 20503

1. AGENCY USE ONLY (Leave blank)	2. REPORT DATE November 18, 1999	3. REPORT Final Report (July 10, ... 99)

4. TITLE AND SUBTITLE New Classes of Ceramic Materials for Thermal Barrier Coating Applications	5. FUNDING NUMBERS AFOSR GRANT F49620-97-1-0498

6. AUTHOR(S)
Sankar Sambasivan

7. PERFORMING ORGANIZATION NAME(S) AND ADDRESS(ES) Northwestern University ACTG 1801 Maple Avenue Evanston, IL 60201-3140	8. PERFORMING ORGANIZATION REPORT NUMBER WW03

9. SPONSORING / MONITORING AGENCY NAME(S) AND ADDRESS(ES) Air Force of Sponsored Research Ceramic Materials	10. SPONSORING / MONITORING AGENCY REPORT NUMBER

11. SUPPLEMENTARY NOTES

12a. DISTRIBUTION / AVAILABILITY STATEMENT **DISTRIBUTION STATEMENT A** Approved for Public Release Distribution Unlimited	12b. DISTRIBUTION CODE

13. ABSTRACT (Maximum 200 Words)

This project investigated the feasibility of using new ceramic materials/concepts for use in thermal barrier coating applications. In one approach, the effect of solid solution on thermal conductivity of refractory spinels (magnesium aluminate-based) was evaluated. Plasma spray process was used to fabricate free-standing discs of spinels with various amounts of cobalt. Preliminary results show that a 2% doping of cobalt in $MgAl_2O_4$ was effective in lowering thermal conductivity. In another approach, the use of layered oxides for TBC applications was explored. Hot pressed samples of potassium calcium niobate (KCN) and another proprietary layered oxide were used to determine the k-T behavior. While both compositions showed significantly low k values (similar to YSZ), KCN decomposed above 1200°C, whereas the second layered oxide was stable at least up to 1400°C. These preliminary results warrant further investigation of such new concepts/materials.

14. SUBJECT TERMS Thermal Conductivity, Thermal Barrier Coatings, Spinel Solid Solutions, Layered Oxides	15. NUMBER OF PAGES 27
	16. PRICE CODE

17. SECURITY CLASSIFICATION OF REPORT Unclassified	18. SECURITY CLASSIFICATION OF THIS PAGE Unclassified	19. SECURITY CLASSIFICATION OF ABSTRACT Unclassified	20. LIMITATION OF ABSTRACT

NSN 7540-01-280-5500

Standard Form 298 (Rev. 2-89)
Prescribed by ANSI Std. Z39-18
298-102

19991208 199

DISTRIBUTION STATEMENT AUTHORIZATION RECORD

Title: *New Classes of Ceramic Materials for Thermal Barrier Coating Applications*

Authorizing Official: *Yvonne Mason*

Agency: *AFOSR*   Ph. No. *(703) 696 - 9518*

☐ Internet Document: URL: _____
(DTIC-OCA Use Only)

Distribution Statement: (Authorized by the source above.)

☒ **A:** Approved for public release, distribution unlimited.

☐ **B:** U. S. Government agencies only. (Fill in reason and date applied). Other requests shall be referred to (Insert controlling office).

☐ **C:** U. S. Government agencies and their contractors. (Fill in reason and date applied). Other requests shall be referred to (Insert controlling office).

☐ **D:** DoD and DoD contractors only. (Fill in reason and date applied). Other requests shall be referred to (Insert controlling office).

☐ **E:** DoD components only. (Fill in reason and date applied). Other requests shall be referred to (Insert controlling office).

☐ **F:** Further dissemination only as directed by (Insert controlling DoD office and date), or higher authority.

☐ **X:** U. S. Government agencies and private individuals or enterprises eligible to obtain export-controlled technical data in accordance with DoD Directive 5230.25.

NOTES: _____

_____

_____

_____

J. Keith _____   *10 Dec 99* _____
DTIC Point of Contact   Date

FINAL REPORT

New Classes of Ceramic Materials for Thermal Barrier Coating Applications

By

Sankar Sambasivan
Northwestern University
ACTG
1801 Maple Avenue
Evanston, IL 60201-3140

Tel: (847) 491-4619
FAX: (847) 467-1022
ssambasivan@nwu.edu

TABLE OF CONTENTS

Table of Figure

EXECUTIVE SUMMARY

Under a one-year AFOSR program, new materials/concepts were evaluated for thermal barrier coating (TBC) applications. In one approach, solid solutions of spinel compounds ($MgAl_2O_4$-based) were evaluated. Undoped spinel ($MgAl_2O_4$) along with 0.5% and 2% cobalt doped spinel compositions were selected for the study. Initial attempts to develop the coatings using a liquid delivery assisted CVD process were not successful. A small particle plasma spray process was used to develop the coatings. Free-standing spinel discs (0.5" diameter; 4-8 mils thick) were fabricated and subjected to thermal conductivity measurements. The as-deposited coatings for doped and undoped spinels exhibited low k values (1-2 W/m.K) due to the presence of pores. Subsequent to the first heat treatment to 1400°C, the coatings sintered and showed typical k-T behavior. However, the k values even for pure spinel were still significantly lower than the reported values in literature. The effect of solid solution on lowering k was more pronounced for the 2% compared to the 0.5% cobalt-doped spinel compositions. These preliminary results suggest that spinels belonging to a broad class of refractory ceramic materials can be potentially useful for TBC applications. The wide compositional range can be used to tailor the thermal, mechanical, and chemical properties of the TBC system. Chromite spinels, for example, are known for their excellent stability against slag or other corrosive environments at elevated temperatures.

In another approach, layered oxides were also evaluated as TBC candidates. The basic premise is that weakly-bonded planes that normally exist between planes containing rigid polyhedra in layered oxides may act as barriers to phonon conduction resulting in lowering of thermal conductivity. Potassium Calcium Niobate ($KCa_2Nb_3O_{10}$) and another layered oxide (proprietary composition) were selected for the study. Bulk samples of these materials were fabricated by hot pressing. Thermal conductivity measurements performed on these materials showed remarkably low k values similar to that observed for yttria stabilized zirconia (RT to 1400°C). While the results are preliminary, this study has shown that layered oxides may serve as potential candidates for TBC applications.

1 INTRODUCTION

Alternate materials/concepts for thermal barrier coating applications were evaluated under a one year program sponsored by the Air Force Office of Scientific Research (AFOSR). The basic objective was to determine the feasibility for lowering thermal conductivity of refractory ceramic compositions through atomistic /microstructural manipulation. Yttria-stabilized zirconia (YSZ) has served adequately well as a thermal barrier coating (TBC) material in many high temperature applications providing a thermal benefit of about 170°C to protect the underlying metal/alloys [1]. It has also provided suitable chemical protection to the metal from the corrosive environments usually encountered in some combustion environments. However, YSZ suffers from two critical drawbacks that causes the TBC coating to spall off resulting in a catastrophic failure of the turbine component [2]. One of the undesirable characteristics of YSZ is its poor creep resistance at high temperatures which induces significant stresses within the coating. These stresses are accommodated through internal cracking of the coating which eventually leads to spallation. The other, rather well known characteristic of YSZ, is the high diffusivity of oxygen at even moderately high temperatures. It is believed that the oxidation of the underlying bond-coat layer is occurring primarily from oxygen diffusion through YSZ. The oxidation products of the bond-coat induce stresses at the bondcoat-TBC interface which also results in spallation of the coating. Such potential for catastrophical failure of turbine components can be especially devastating for Air Force applications. Therefore, it is prudent to explore other ceramic compositions that will replace YSZ as a TBC material which can provide the thermal benefits offered by YSZ and at the same time be robust in its resistance to creep, corrosion, and oxygen diffusivity.

In one approach, solid solution effects on thermal conductivity (k values) was evaluated using AB_2O_4-type spinel compositions. Spinel compounds (e.g., $MgAl_2O_4$) belong to a broad family of refractory compositions with desirable physical and chemical properties for TBC applications (Table I). They are used extensively as refractories in metal and ore processing due to their excellent corrosion resistance to molten slags and corrosive

vapors. They possess an extensive solid solution range which provides an opportunity to tailor coefficients of thermal expansion (CTE ranges from 9-12.10^{-6} /K), chemical properties for adequate corrosion protection, and chemical compatibility with underlying bondcoat/substrate. Previous work on simple oxide solid solutions (MgO-NiO) have shown that solute content can influence k values significantly (Figure 1)[3]. The magnitude of the solid solution effect is dictated by several factors including atomic size difference between solute and host ion, bond energy differences, and the elastic strain fields around the substituted atom.

Table I. Selected Spinel Compositions and Properties.

Composition (AB$_2$O$_4$)	Melting Point (°C)	Thermal Expansion (.10^{-6}/°C)	A^{2+}radii (Å)	B^{3+}radii (Å)	| r$_{Mg}$-r$_A$ ||	| r$_{Al}$-r$_B$ ||
MgAl$_2$O$_4$	2130	7.8	0.86	0.62	—	—
MgFe$_2$O$_4$	1750	12.11	0.86	0.75	—	0.08
CoAl$_2$O$_4$	—	8.5	0.76	0.67	0.10	—
MnAl$_2$O$_4$	—	7.2	0.81	0.67	0.05	—
NiAl$_2$O$_4$	2020	8.4	0.84	0.67	0.02	—
MgCr$_2$O$_4$	2000	7.9	0.86	0.76	—	0.09
ZnAl$_2$O$_4$	1950	8.7	0.89	0.67	0.03	—
MnCr$_2$O$_4$	—	9.3	0.81	0.76	0.05	0.09
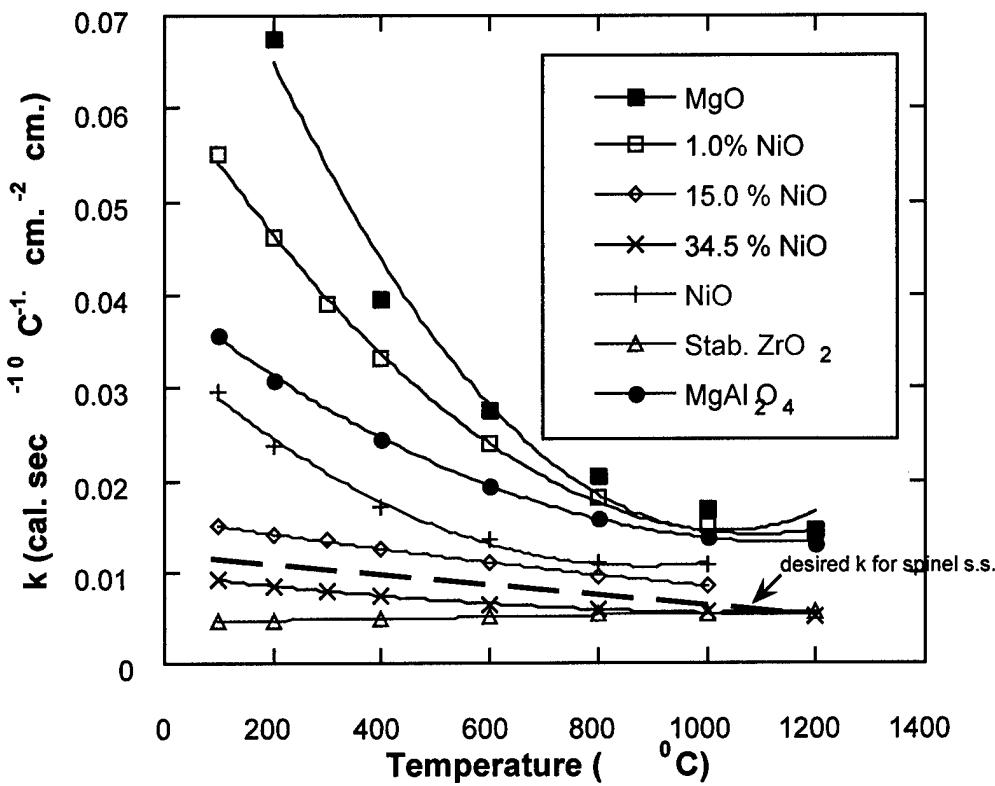
(Kingery W.D., J. Am. Ceram. Soc., 42[12](1959)617-27)

Figure 1. Thermal Conductivity Behavior in oxide systems.

Several key features of this plot are noteworthy:

1) Both 15 & 34.5 mol% NiO-containing samples have significantly lower k values than their corresponding pure MgO and NiO.

2) As the NiO concentration in MgO is increased, the k values become less temperature dependent.

3) At temperatures above 600°C, k-T relationship of 34.5 mol% NiO samples is very similar to that of stabilized zirconia.

In theory, the solid solution effect is expected to be much less pronounced at elevated temperatures (above Debye T) due to dominant scattering effects from intrinsic lattice vibrations [4]. However, the MgO-NiO study suggests that solid solutions can be

4

sufficiently effective in lowering thermal conductivity even at high temperatures (compare 34.5 mole % NiO-MgO with stabilized zirconia in Figure 1). This effect has not been explored or studied in any detail. On the other hand, recent work on garnets shows the solid solution effect to be minimal [5]. In general, complex or multi-cation chemistries induce significant intrinsic lattice disorder resulting in relatively low thermal conductivity such that solid solution effects are minimized[6]. Spinels are isotropic in nature with excellent high temperature properties for corrosion resistance, low oxygen mobility, creep resistance, and relatively high thermal expansion coefficients to match the superalloy-based substrate materials. Although spinels are not known to be as good in resisting phonon conduction as YSZ, it is anticipated that the effect of incorporating substituional cations may be significant enough to match "k" values offered by YSZ (at least above 1200°C). They possess an extensive solid solution range which provides an opportunity to tailor coefficients of thermal expansion (CTE ranges from $9\text{-}12.10^{-6}$ /K), chemical properties for adequate corrosion protection, and chemical compatibility with underlying bondcoat/substrate. However, as these simple oxides (NiO, MgO) are environmentally not suitable for TBC applications, other solid solution systems will have to be explored.

In another approach, materials with a high degree of crystalline anisotropy (such as layered perovskites or layered spinels) were evaluated. The basic premise is that weakly-bonded planes that normally exist between planes containing rigid polyhedra in layered oxides may act as barriers to phonon conduction resulting in lowering of thermal conductivity. Any disruption or disorder that decreases the mean free path for phonon conduction is potentially useful for lowering thermal conductivity. The weakly-bonded planes in layered oxides can be termed as "atomically" disordered planes and may be useful. Based on our limited mechanical tests on hot pressed samples of potassium calcium niobate ($KCa_2Nb_3O_{10}$ or KCN), a layered perovskite, it appears that the intralayer mirror planes are very compliant and flexible in accommodating slight changes in local chemistry [7]. Our experiments of indentation on large grains of KCN show that multiple cracks form readily along the basal planes with no apparent cracks forming along the c-axis, under a modest load of 25g (Figure 2). These materials are often termed

as "soft" ceramics for their extreme sensitivity to plastic damage under such relatively small loads. It is emphasized that KCN, in this study, is only being considered to demonstrate feasibility of this approach and that other suitable compositions may have to be considered for the actual application.
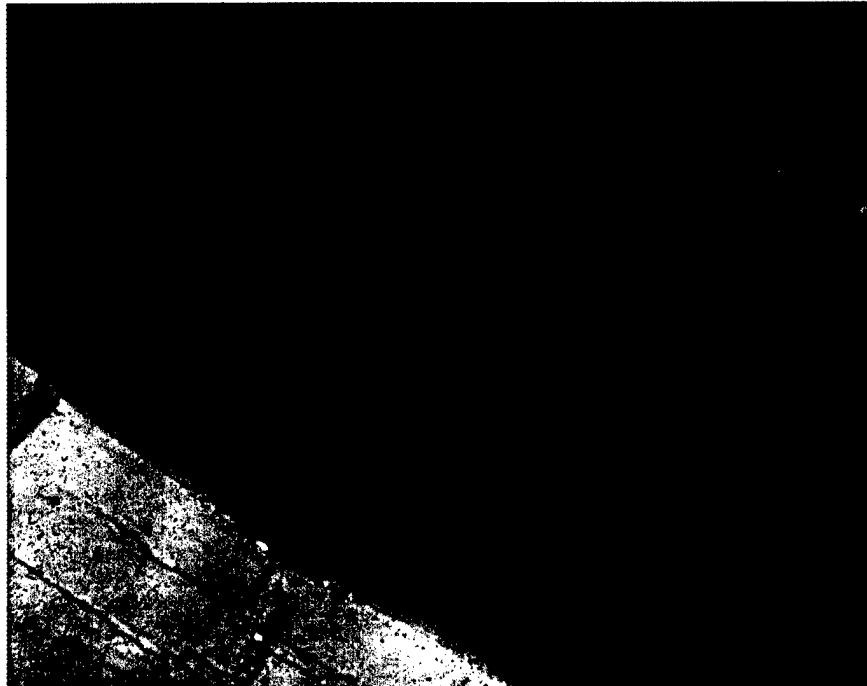

Figure 2. Vickers Indentation on KCN.

The general idea is not new. The concept has been evaluated at a much "coarser" scale through the use of many alternate layers of alumina and zirconia where the interfaces between the layers act as barriers to phonon conduction [8]. However, the results showed that the effect of these interfaces was not significant, suggesting that extremely thin layers may be necessary to derive the benefit. The use of highly anisotropic materials offer the ability to introduce " layered" disorder at the atomic scale. In addition, these layered oxides also exhibit a high degree of anisotropy in thermal expansion. For example, potassium calcium niobate ($KCa_2Nb_3O_{10}$), a layered perovskite, has a CTE value of 7.10^{-06}/K in the a-direction and 20.10^{-07}/K in the c-direction [9]. This property is

useful and allows for minimizing residual stresses by controlling the CTE through the degree of texture in the coating. Its fracture behavior is unique and provides further evidence on the extent of crystalline anisotropy.

2   <u>EXPERIMENTAL SECTION</u>

Based on the proposed plan to develop these coatings by a liquid delivery assisted CVD process, deposition equipment was set-up and built using a COVA flash evaporator system. A hot wall CVD reactor was set-up and attached to the COVA flash evaporator (Figure 3). Magnesium aluminum double isopropoxide was used as the liquid precursor source (Chemat Technology, Inc.). As the COVA system has not be fully optimized by the supplier, severe problems were encountered during the development. After many trial experiments, the decision was made to pursue the coating development using a plasma spray process.
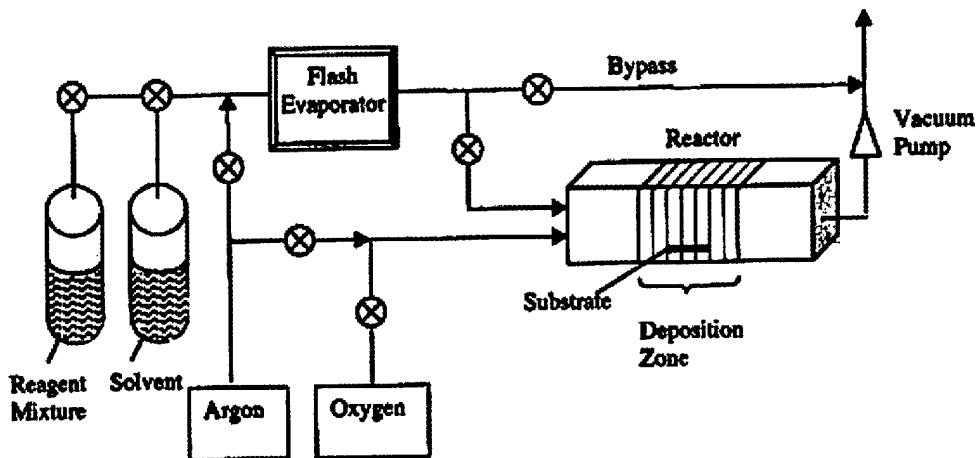
Figure 3. Schematic Diagram of the Liquid Delivery-Assisted CVD System

For concept demonstration, magnesium aluminate spinel ($MgAl_2O_4$) along with 0.5 and 2 mole % cobalt (II) compositions were selected for the study. The divalent cobalt ion substitutes for magnesium in the spinel structure to form normal spinel solid solutions. Powders of all three compositions were obtained from McDermott Technology Inc.

7

(courtesy of Richard Goettler) and characterized by x-ray diffraction to confirm spinel as the only phase present. Coatings of spinel and its solid solutions were developed on metal substrates by small particle plasma spray (SPPS) process. The coatings were etched out from the substrates to yield free-standing discs. Figure 4 is a SEM micrograph in cross-section of the 2% cobalt-doped spinel. After confirming the spinel phases by XRD, the free-standing discs were subsequently delivered to Holometrix, Inc. for measurement of thermal conductivity (RT to 1400°C, see Appendix A). The samples were held for 15 minutes at each temperature during the heat-up and cool-down cycle.
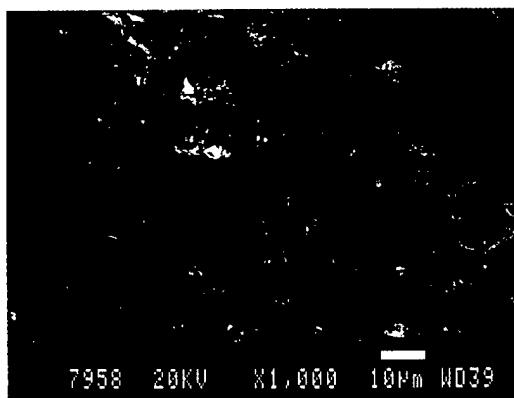
Figure 4 SEM mage of as -deposited spinel (2% cobalt) coatings by Plasma Spray.

For the layered oxides, bulk specimens of textured potassium calcium niobate and another layered oxide (proprietary composition) were prepared by hot pressing (prepared under a previous AFOSR program) which yielded 'a' and 'c' textured specimens for thermal conductivity measurements. Powders of both layered oxide materials were synthesized by Petuskey and coworkers at Arizona State University.

3   RESULTS AND DISCUSSION

3.1   Spinel Solid Solutions

The results obtained from thermal conductivity measurements on spinel solid solutions
are summarized below:

1. The k-T behavior for all three samples were typical of plasma-sprayed coatings
    (Figure 5a). During the first heat-up cycle, all three samples exhibited low k values
    up to 1200°C followed by an increase at higher temperatures due to sintering of the
    plasma sprayed deposits. While a high level of porosity is observed for the as-
    deposited coatings, significant sintering appears to have occurred upon heat
    treatment. The behavior during the cool-down cycle represented that of typical
    ceramic materials (k decreases with temperature due to umklapp scattering effects).
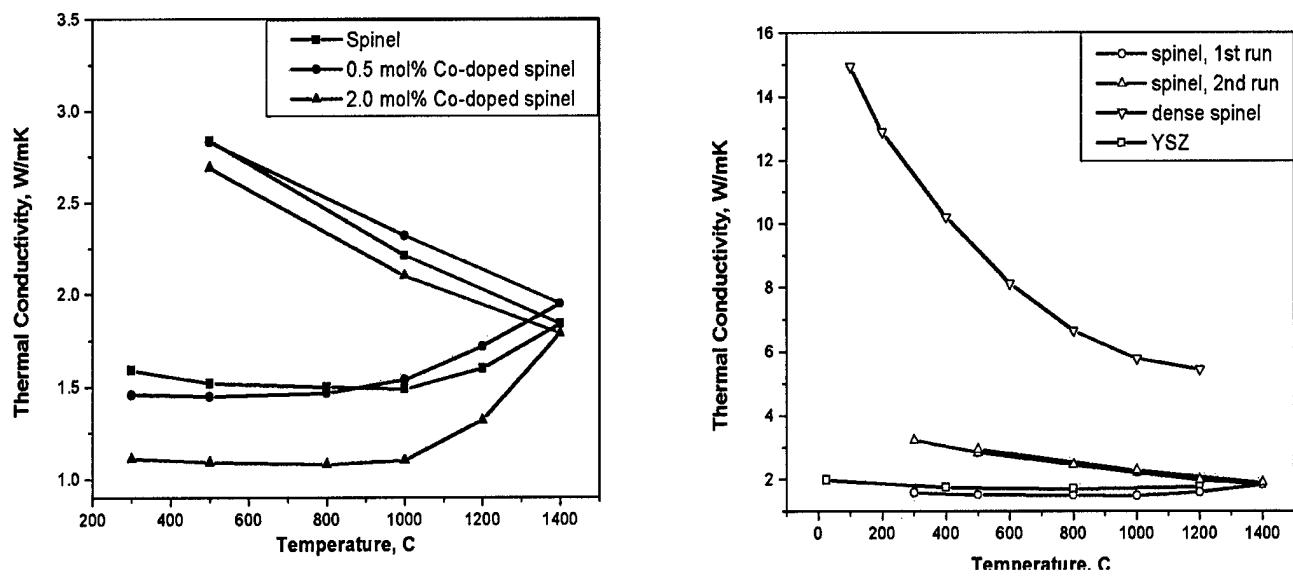
**Figure 5. Thermal conductivity behavior of spinels: comparison of pure and doped
spinels (left); comparison of pure dense spinel with YSZ and plasma   sprayed
spinel.**

2. In an attempt to test the microstructural stability of the "sintered" plasma sprayed coatings after the first heating run, the undoped spinel sample was subjected to a second run where the k-T curve followed the profile of the cool-down cycle from the first run suggesting the coatings to be microstructurally stable (Figure 5b).

3. Thermal conductivity of plasma-sprayed spinel and cobalt-doped materials was significantly lower than the reported value for pure dense spinel over the entire temperature range (Figure 5b). Based on density measurements of the free-standing discs and SEM evaluation of the coatings in cross-section, it can be inferred that the material contains finely distributed porosity which may have contributed to low k values. If the pore structure can be stabilized, the coating may be quite effective in resisting phonon conduction.

4. While little or no difference in k values was observed for the 0.5 mole % cobalt-doped sample as compared to undoped spinel, a finite difference in k value was observed for the 2 mole% cobalt-doped spinel (larger difference below 1000°C).

Figure 6 shows the TEM micrographs (plan view) of as-deposited (~25% porosity) and annealed (samples prepared after thermal conductivity measurements) spinel coatings.
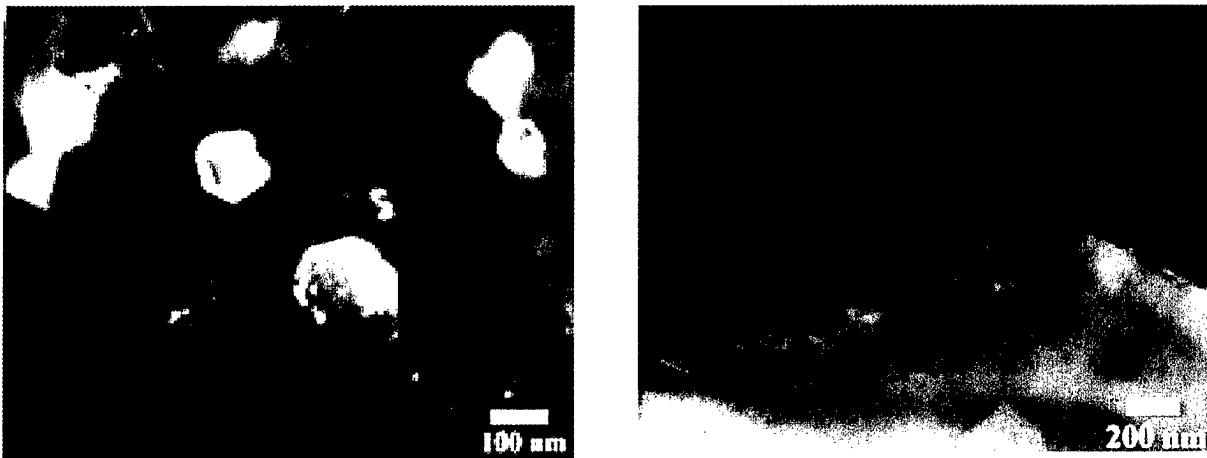
Figure 6. Spinel Coatings Developed by Plasma Spray; as-deposited (left); annealed to 1400°C (right).

While further work is warranted, these results clearly suggest that spinel compositions are attractive candidates for TBC applications and that both atomistic (through solid solution)

10

and microstructural (through fine porosity) tailoring can offer desirable thermal, chemical, and mechanical properties. Spinel compounds can be accommodated with much higher solute contents of several elements in both cationic sublattices which should provide even much higher resistance to phonon conduction.

3.2 Layered Oxides

For $KCa_2Nb_3O_{10}$, thermal conductivity measurements were done on both crystallographic directions (a & c). Although, k values were low in both directions, the k value in the c-direction (across the weakly bonded planes) was much lower than in the a-direction (within the perovskite block). However, the material was tested under conditions where it decomposed resulting in anamolously high k values at temperatures above 1200°C (Figure 7a). The approach was also tested with another layered oxide which was prepared by hot pressing. The k-T behavior for this material (in the hot pressing direction) is shown in Figure 7b (2 runs conducted) where this phase appears to be stable well over 1300°C. Unlike other monolithic ceramic materials, the profile is flat and similar to YSZ where the presence of extrinsic point defects (oxygen vacancies and yttrium substitutions) dictate the k-T behavior. In this case, it appears that the presence of weakly-bonded planes do act as barriers for phonon conduction over the entire temperature range which is quite interesting. It is also worth noting that the k value actually drops even further at temperatures above 1200°C.

These results show that highly anisotropic materials hold great promise as candidates for TBCs. It will certainly be interesting to explore this concept further and determine whether it is feasible to develop a matured TBC system using these materials that exhibit unique thermal and physical properties.
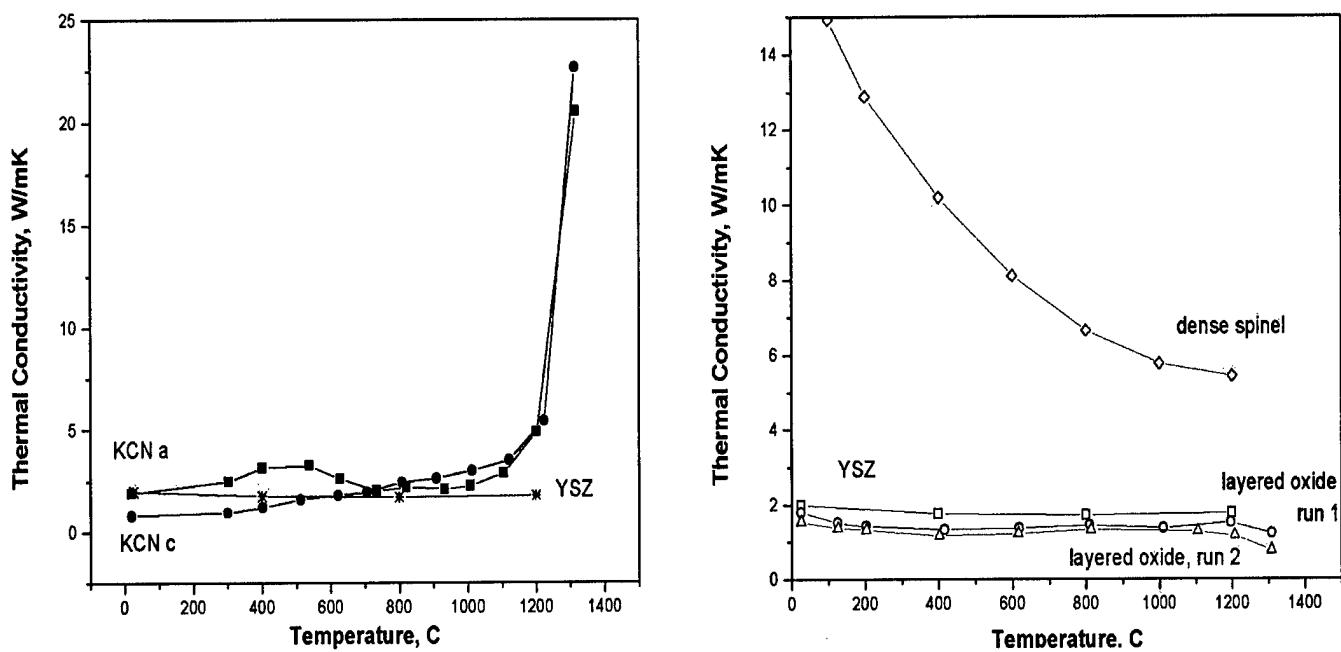
Figure 7. Thermal conductivity behavior of anisotropic materials; hot pressed potassium calcium niobate (left); hot pressed layered oxide (right).

Layered oxide materials are also attractive for inducing strain tolerance in TBC systems. Due to the compliant nature of the material, thermally induced stresses are accommodated through plastic deformation. Figure 8 is a TEM cross-sectional micrograph of annealed sample of a layered oxide (proprietary composition) used in this study. Two points are noteworthy from the TEM studies: a) As shown in Figure 7a (right), the disorder across the layers appears to be extensive at the "atomic level" from stresses induced during thermal cycling. This may be beneficial in further reducing thermal conductivity, b) the TEM micrograph in Figure 7b (left) shows a grain bent (almost at right angles) due to thermal stresses induced during heat treatment. The severe plastic deformation observed suggests a high degree of compliance to exist in these materials. These results appear promising and raises the realistic possibility for incorporation of layered oxides in TBC applications.

12
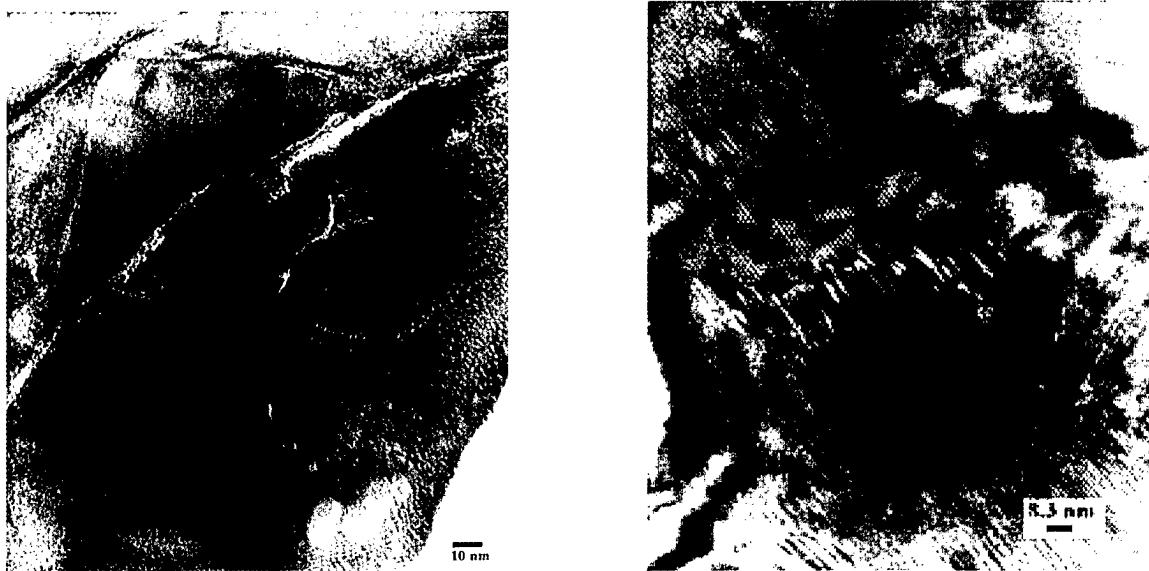
Figure 8. TEM micrograph of layered oxide ; plastically deformed grain (left); highly disordered grain (right).

4   REFERENCES

1. R. A. Miller, "Thermal Barrier Coatings for Aircraft Engines - History and Directions", Thermal Barrier Coating Workshop, March 1995, NASA Conference Publication 3312.

2. W. J. Brindley, "TBC R&D Issues for Gas Turbine Engines", Presented at ATS Materials Workshop, Charleston, SC February 1996.

3. W.D. Kingery, "Thermal Conductivity: XIV, Conductivity of Multi-Component Systems, J. Am. Ceram. Soc., **42**[12] (1959) 617-28.

4. W.D. Kingery, H.K. Bowen, and D.R. Uhlmann, "Introduction to Ceramics", IInd Ed., John Wiley & Sons, New York, 1976, pp 636-43.

5. N.P. Padture, P.G. Clemens, "Low Thermal Conductivity in Garnets", J. Am. Ceram. Soc., **80**[4] (1997) 1018-20.

6. W.D. Kingery, H.K. Bowen, and D.R. Uhlmann, "Introduction to Ceramics", IInd Ed., John Wiley & Sons, New York, 1976, pp 621-4.

7. S.T. Kim, V.P. Dravid, and S. Sambasivan, "Chemical and Morphological Analysis of Sol-derived $KCa_2Nb_3O_{10}$, J. Mater, Res., Vol. 14, No. 4 (1999) 1325-1328.

8. K.S. Ravichandran, K. An, R.E. Dutton, S.L. Semiatin, "Thermal Conductivity of Plasma Sprayed Monolithic and Multilayer Coatings of Alumina and Yttria-Stabilized Zirconia", J. Am. Ceram. Soc., 82[3] (1999) 673-82.

9. K. Steiner, M.S. Thesis, Arizona State University, Tempe, AZ (1998).

5 ACKNOWLEDGEMENT

6 KEY PERSONNEL

Dr. Sankar Sambasivan - PI

Ms. Kimberly Steiner - Research Scientist (processing & Characterization)

Dr. Zhen Liu - Postdoctoral Associate (TEM characterization)

Mr. Benjamin Goldsmith - Undergraduate Student (Cooperative Education Internship Program) - CVD set-up

7 PUBLICATIONS, PRESENATATION AND INVENTION

1. S. Sambasivan and K. Steiner, "New concepts and materials for TBC applications," poster presented at the Annual meeting of the American Ceramic Society meeting, Indianapolis, IN, May 1999.
2. Invention disclosure filed on "Highly Anisotropic Ceramic Compounds as Thermal Barrier Coating Materials," NU Invention No. 99036.

Report on the

Thermal Diffusivity, Specific Heat, and Thermal Conductivity of Ceramic Coatings

This report presents the results of thermal diffusivity, specific heat and calculated thermal conductivity measurements of three ceramic coating samples submitted by Northwestern.

The samples, identified as A, B and C were submitted as free-standing disks approximately 12.7 mm diameter by 0.2 mm thick.

Thermal diffusivity and specific heat were measured at 300, 500, 800, 1000, 1200 and 1400°C by the laser flash method utilizing a Holometrix Thermaflash 2200 instrument. This instrument and method conform to ASTM E1461-92, "Standard Test Method for Thermal Diffusivity of Solids by the Flash Method" for the measurement of thermal diffusivity. The method for the measurement of specific heat by laser flash is described below.

The test results are given after a description of the experimental procedure.

Thermal Diffusivity

Transient heat transfer problems occur when the temperature distribution changes with time. The fundamental quantity that enters into heat transfer situations not at steady-state is the thermal diffusivity. It is related to the steady-state thermal conductivity through the equation

$$D = \frac{\lambda}{C_p \rho} \tag{1}$$

where D is the thermal diffusivity, λ is the thermal conductivity, C_p is the specific heat, and ρ is the density. The diffusivity is a measure of how quickly a body can change its temperature; it increases with the ability of a body to conduct heat (λ) and it decreases with the amount of heat needed to change the temperature of a body (C_p). All three quantities on the right hand side of Equation (1), as well as the thermal diffusivity, can be functions of temperature.

Thermal properties of materials are measured by experimentally establishing a heat flow boundary value problem, solving the theoretical equations, and then measuring the

necessary temperatures or heat fluxes to determine the thermal property by matching to the theoretical solution. Thus the easiest theoretical way to measure the thermal conductivity is to set up a steady-state, linear flow of heat through the material and apply Fourier's equation. This approach has led to the development of a number of methods for measuring the thermal conductivity including the Guarded Hot Plate and Linear Rod methods. These methods are time consuming and can be susceptible to errors arising from non-realization of the assumed boundary or steady-state conditions. The flash methods of measuring thermal diffusivity remove the steady-state condition at the expense of measuring temperature as a varying function of time.

The measurement of the thermal diffusivity of a material is usually carried out by rapidly heating one side of a sample and measuring the temperature rise curve on the opposite side. The time that it takes for the heat to travel through the sample and cause the temperature to rise on the rear face can be used to measure the through-plane diffusivity and calculate the through-plane thermal conductivity if the specific heat and density are known. The through-plane measurement is depicted in Figure 1.
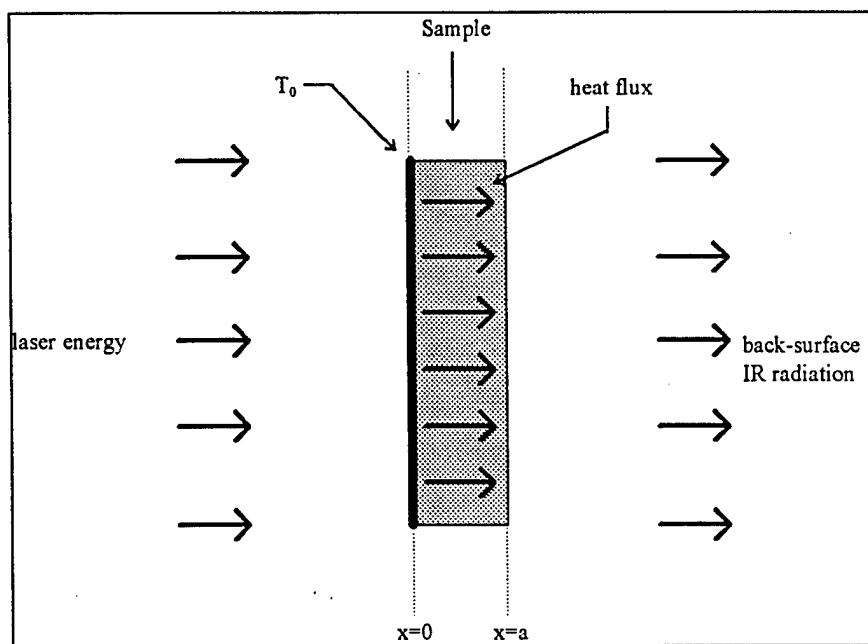

Figure 1

Through-Plane Method and Analysis

The basic method is sketched in Figure 2. The sample is a disk with a standard diameter of 12.7 mm and a thickness ranging from about 0.1 to 3 mm. With the Holometrix Thermaflash 2200 Laser Flash system, the sample disk is aligned between a neodymium

glass laser (1.06 µm wavelength) and an indium antimonide (InSb) IR detector in a tantalum tube furnace. A Type C thermocouple in contact with the sample controls the sample and its surroundings at any temperature between 20 and 2000°C. Once the sample has been stabilized at the desired temperature, the laser is fired several times over a span of a few minutes and the necessary data is recorded for each laser "shot". The laser beam energy strikes and is absorbed by the front surface of the sample, causing a heat pulse to travel through the samples' thickness. The resulting sample temperature rise is fairly small, ranging from about 0.5 to 2 degrees C. This temperature rise is kept in the optimum range by adjustable filters between the laser and the furnace. A lens focuses the back surface image of the sample onto the detector and the temperature rise signal vs. time is amplified and recorded with a high speed A/D converter. Figure 3 is an example of an actual temperature rise curve.
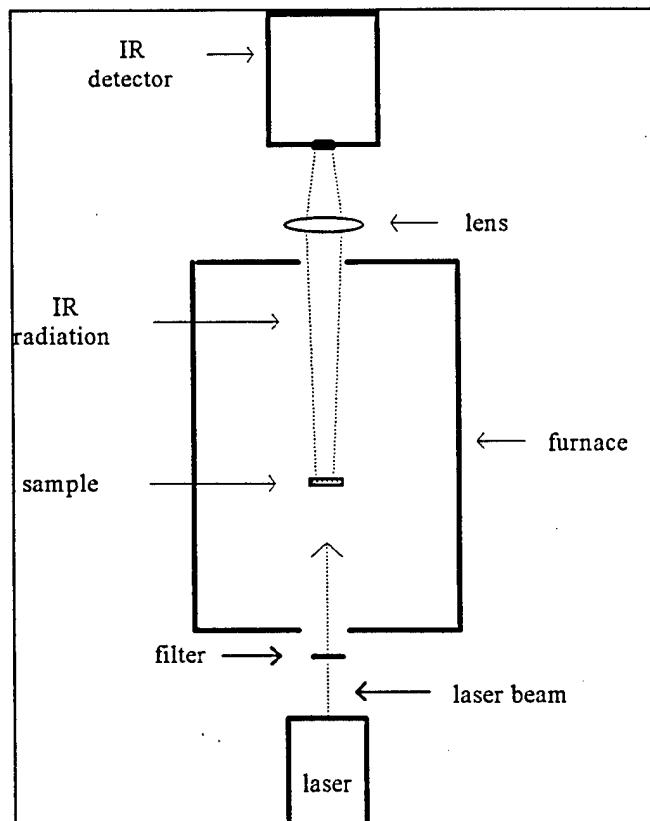
Figure 2

Testing is performed in a high vacuum or inert gas environment. The instrument is fully automated to control all systems and record, analyze and report the thermal diffusivity, specific heat and the calculated thermal conductivity.

The Holometrix Microflash system, designed for measurements from room temperature to 300°C, utilizes a lower temperature furnace design and lacks a vacuum system for controlling the furnace environment.

Samples that do not naturally have a high value of emissivity or absorbtivity are coated with a graphite film before testing. The graphite increases the energy absorbed on the laser side and increases the temperature signal on the back side of the sample. Some materials are transparent to infrared radiation and must be coated with a metal film on both sides. This prevents penetration of the laser beam into the sample on the front side, and on the back side it prevents the viewing of the IR detector into the sample. A 1000 Å gold film can be used as it constitutes many skin depths at the frequency of the laser or of the thermal radiation from the sample.
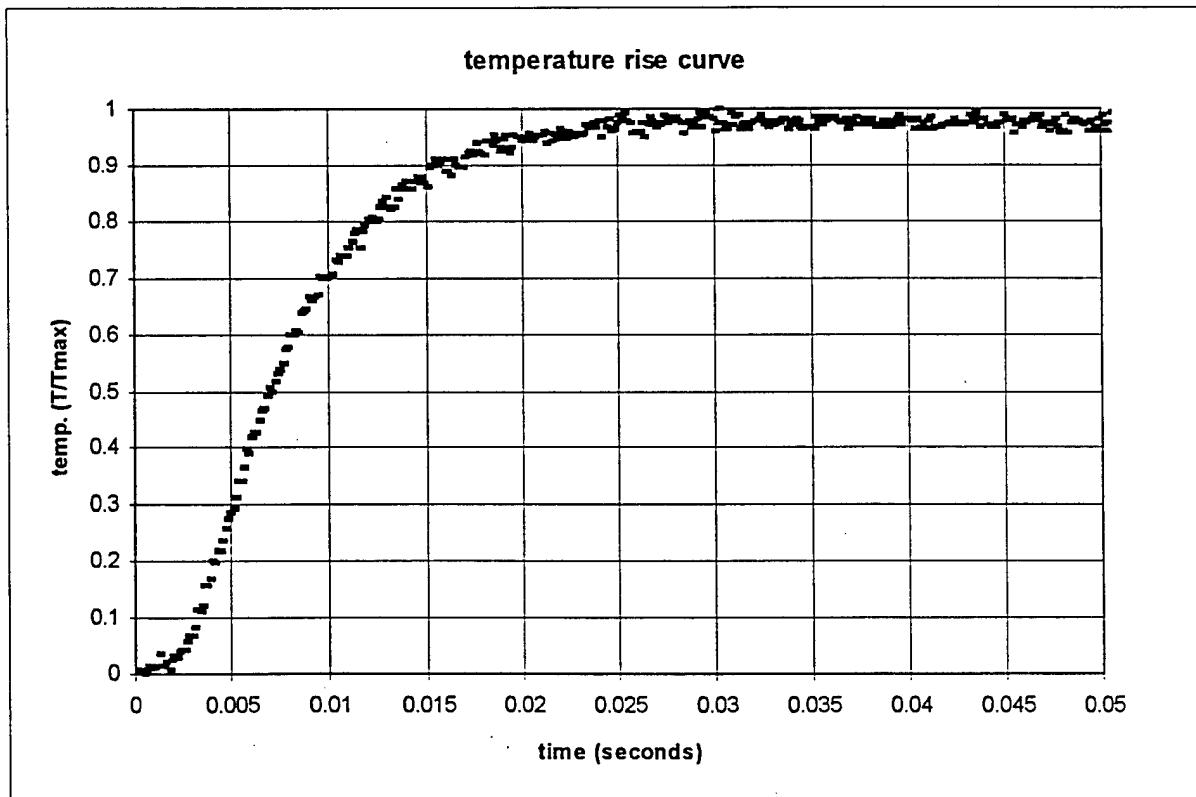
Figure 3

For measurements below room temperature, the Thermaflash 2200 system is adapted with a cryogenic testing cell. The cell uses a liquid nitrogen flow to cool a heat sink and the sample down to approximately -170°C, and a resistance heater to re-heat and control at intermediate temperatures. A type K thermocouple in contact with the sample provides control feedback. At temperatures between 25°C and about -75°C, a Mercury-Cadmium-

Telluride IR detector can be used to measure the back surface temperature rise. At lower temperatures it is necessary to use a thermocouple in contact with the back surface because the detector sensitivity is not adequate. Various methods can be used to attach the thermocouple, but the response time of the thermocouple must be much faster than the temperature rise of the back surface. Thermocouple wire with a small diameter, high sensitivity and low thermal conductivity is typically used to achieve a fast response and adequate signal to noise ratio (1 or 2 mil type E, for example). For electrically conducting materials, an intrinsic arrangement can be used with each leg tack welded directly to the sample. For other materials, a thin film of gold is first deposited on the surface and the wires are pressed or taped to the surface. The response time of thermocouple is verified by comparing to measurements made with the IR detector at the same sample temperature.

In the through-plane measurement depicted in Figure 1, the sample can be thought of as part of a sheet of material infinite in two dimensions but of finite thickness. Before the flash, the temperature of the sample and surroundings is at some uniform temperature that can be taken as zero. Immediately after the flash, the front surface of the sample is at some higher temperature, T_0. The heat flux lines are parallel and directed through the sample; there is no heat flow in the plane of the sample. The boundary conditions consist of radiation heat transfer from the front and rear faces into a surrounding space at the initial zero temperature. There have been many solutions of this boundary/initial value heat equation problem in different forms. The first to apply the solution to the flash diffusivity measurement was Parker et al.[1] Using the notation of Koski[2], the resulting equation for the rear face temperature as a function of time is

$$T(a,t) = 2T_f \sum_{n=1}^{\infty} \frac{\gamma_n^2(\gamma_n^2 + L^2)\cos\gamma_n}{\gamma_n^2 + L^2 + 2L} \exp(-\gamma_n^2 Dt/a^2) \qquad (2)$$

where

T_f	=	the final adiabatic sample temperature
D	=	the thermal diffusivity
t	=	time
a	=	the sample thickness
L	=	the heat loss factor

Each γ_n is found by solving the transcendental equation

$$\tan \gamma_n = \frac{2\gamma_n L}{\gamma_n^2 - L^2} \qquad (3)$$

The finite width of the laser pulse, t_p, can affect the measurement of thin and/or high diffusivity samples because the heating of the front surface can no longer be considered instantaneous relative to the time for the heat to diffuse through the sample. To include this effect in the analysis, the laser pulse width is folded into the results by convoluting Equation (2) with the pulse shape. If there is no heat loss, i.e. L=0, and the finite pulse can be ignored, then Equation (2) leads to the Parker expression

$$D = \frac{0.139a^2}{t_{50}} \qquad (4)$$

where t_{50}, the half rise time, is the time for the back face temperature to reach 50% of its maximum value. The constant value of 0.139 is known as the Fourier number. Equation (4) is a very useful expression for calculating optimum sample thickness and expected rise times if the approximate diffusivity is known.

In the more general case, the approach used is that of Koski.[2] Equation (2) can be used to generate the temperature rise curve if the diffusivity and the loss factor are known. The analysis of the laser flash data requires the inverse of this operation; the temperature rise curve is known and the diffusivity is to be determined. The time required to perform real time analysis of the laser flash data can be reduced by pre-establishing the relationship between the diffusivity, loss factor and pulse width correction and the shape of the temperature rise curve. Koski generated the temperature rise curves for a large range of diffusivity and heat loss and then analyzed the curves for their shapes. There are a number of parameters that can be used to describe the shape of the curve; Koski considers two approaches, that of Clark and Taylor[3] and that of Cowan[4]. Both use the ratio of the pulse width to the half rise time, $r_1 = t_p/t_{50}$, as one parameter. Cowan (as applied by Koski) uses as a measure of the heat loss a second parameter, r_2, the ratio of the temperature at five times t_{50} to the temperature at t_{50}. Clark and Taylor prefer to use only that part of the temperature rise curve before the peak. They noted that heat loss causes the curve to rise more steeply, so they use as r_2 the ratio of t_x to t_y, where x and y are percentages of the maximum temperature rise. Koski considers three ratios: t_{70}/t_{30}, t_{80}/t_{20}, t_{80}/t_{40}. One of these ratios is used along with r_1 as the two parameters that define the shape of the curve. Surface fits were made to the diffusivity and loss factor. The fits are a method of interpolating for shape parameters that do not correspond exactly to one of the temperature rise curves generated in the study.

Holometrix

The data is analyzed using both the Clark and Taylor method and the Cowan method. Because data taken on real samples does not conform exactly to the assumptions made in the theoretical analysis, either the Clark and Taylor method or the Cowan method may give better agreement with the data. After each laser shot the analyzed time rise curve is plotted and compared to the theoretical curve having the same value of diffusivity and heat loss. The software used in the analysis was verified by analyzing curves with known values of diffusivity and heat loss. All resultant values of diffusivity were within 1 % of the input values.

Specific Heat

The specific heat of a material is defined as the amount of energy required to raise a unit mass of material by one unit of temperature at constant pressure.

$$Cp = \frac{Q}{m\Delta T}$$

where:

Cp = specific heat

m = mass

ΔT = change in temperature

Q = energy

Specific heat can be measured with the laser flash method by comparing the temperature rise of the sample to the temperature rise of a reference sample of known specific heat tested under the same conditions[1]. This temperature (voltage) rise is recorded during the diffusivity measurement, so the specific heat can be calculated from the same data with a suitable calibration. Assuming that the laser pulse energy and its coupling to the sample remain essentially unchanged between samples:

$$Q = \text{absorbed energy} = (mCp\Delta T)_{ref} = (mCp\Delta T)_{sample}$$

and:

$$Cp_{sample} = \frac{(mCp\Delta T)_{ref}}{(m\Delta T)_{sample}} = \frac{(mCp\Delta V)_{ref}G_{sample}}{(m\Delta V)_{sample}G_{ref}} \tag{5}$$

A reference sample is measured at each temperature of interest to calibrate the change in output voltage of the IR detector (ΔV) resulting from the absorbed laser energy. The

measured ΔV divided by the detector amplifier gain (G) will be proportional to the temperature rise (ΔT), as long as the temperature rise is small. This calibration gives the absorbed energy or calibration factor in terms of the mass, specific heat, ΔV and G for the reference sample measurement. When a sample of unknown specific heat is measured, the absorbed energy divided by the product of the mass and $\Delta V/G$ of the test sample, Equation 5, gives the test sample specific heat.

The measured ΔV will be affected by heat loss during the measurement, so in order to use ratios of the measured ΔV in Equation 5, the heat loss factors (see Equation 2) of the reference and test sample should be similar. Testing has shown that the laser pulse energy is stable from pulse to pulse within about $\pm 2\%$, so the average of several laser pulses at each temperature are used in the calculations. The absorptive efficiency of the front surface of the samples to the laser pulse and the radiative efficiency of the back surface to the IR detector are controlled by coating the reference and test samples with the same thin layer of graphite.

Conductivity

The sample thermal conductivity can be calculated with Equation (1), after a measurement of the diffusivity and specific heat as described above, and with a measurement of the sample bulk density. The bulk density is normally calculated from the sample dimensions and mass.

Test Results

The measured values of thickness, bulk density, specific heat, thermal diffusivity and the calculated thermal conductivity are given in Table 1 and the thermal conductivity vs. temperature is plotted in Figure 4. Measurements were made during the sample cool down to check for changes due to heat treatment. The results have not been corrected for thermal expansion. The samples were coated with approximately 0.1 μm of gold and 5 μm of graphite for testing. The diffusivity and specific heat values are estimated to be accurate to within $\pm 5\text{-}7\%$, the bulk density values within $\pm 5\%$ and the calculated conductivity values within $\pm 9\text{-}11\%$.

Holometrix

References

1. W.J. Parker, R.J. Jenkins, C.P. Butler, and G.L. Abbott, "A Flash Method of Determining Thermal Diffusivity, Heat Capacity, and Thermal Conductivity", J. Appl. Phys. **32**, 1679 (1961)

2. J.A. Koski, "Improved Data Reduction Methods for Laser Pulse Diffusivity Determination with the Use of Minicomputers", in Proc. Eighth Symp. Thermophysical Prop., Vol II, J.V. Sengers, Ed, Amer. Soc. Mech. Eng., New York (1981).

3. L.M. Clark III and R.E. Taylor, "Radiation Loss in the Flash Method for Thermal Diffusivity", J. Appl. Phys. **46**, 714-719 (1975).

4. R.D. Cowan, "Pulse Method of Measuring Thermal Diffusivity at High Temperature", J. Appl. Phys. **34**, 926-927 (1963).

Holometrix

Table 1

Laser Flash Thermal Conductivity Results

Sample	thickness @ 25°C (mm)	bulk density ρ @ 25°C (g/cm³)	temperature (°C)	specific heat Cp (J/gK)	diffusivity α (cm²/s)	conductivity λ (W/mK)
A	0.170	2.14	300	1.13	0.00655	1.59
			500	1.22	0.00584	1.52
			800	1.31	0.00535	1.50
			1000	1.36	0.00514	1.49
			1200	1.37	0.00547	1.60
			1400	1.39	0.00621	1.84
		on cooling	1000	1.36	0.00761	2.21
			500	1.22	0.0109	2.84
B	0.294	2.40	300	1.14	0.00537	1.46
			500	1.23	0.00492	1.45
			800	1.32	0.00464	1.47
			1000	1.41	0.00458	1.54
			1200	1.42	0.00507	1.72
			1400	1.43	0.00568	1.95
		on cooling	1000	1.41	0.00687	2.32
			500	1.23	0.00962	2.83
C	0.396	2.61	300	1.16	0.00368	1.11
			500	1.26	0.00333	1.09
			800	1.36	0.00304	1.08
			1000	1.39	0.00304	1.10
			1200	1.41	0.00358	1.32
			1400	1.42	0.00482	1.79
		on cooling	1000	1.39	0.00578	2.10
			500	1.26	0.00818	2.69